Cerebellar dentate nucleus functional connectivity with cerebral cortex in Alzheimer's disease and memory: a seed-based approach

Cerebellar dentate nucleus functional connectivity with cerebral cortex in Alzheimer's disease and memory: a seed-based approach

Giusy Olivito 1, Laura Serra 2, Camillo Marra 3, Carlotta Di Domenico 2, Carlo Caltagirone 4, Sofia Toniolo 2, Mara Cercignani 5, Maria Leggio 6, Marco Bozzali 5

1Department of Psychology, Sapienza University of Rome, Rome, Italy; Ataxia Laboratory, Fondazione Santa Lucia-IRCCS, Rome, Italy; Neuroimaging Laboratory, Fondazione Santa Lucia-IRCCS, Rome, Italy. Electronic address: g.olivito@hsantalucia.it.

2Neuroimaging Laboratory, Fondazione Santa Lucia-IRCCS, Rome, Italy.

3Università Cattolica del Sacro Cuore, Fondazione Policlinico Agostino Gemelli-IRCCS, Rome, Italy.

4Department of Clinical and Behavioural Neurology, Fondazione Santa Lucia-IRCCS, Rome, Italy; Department of Systems Medicine, University of Rome 'Tor Vergata', Rome, Italy.

5Neuroimaging Laboratory, Fondazione Santa Lucia-IRCCS, Rome, Italy; Clinical Imaging Sciences Center, Brighton and Sussex Medical School, Brighton, UK.

6Department of Psychology, Sapienza University of Rome, Rome, Italy; Ataxia Laboratory, Fondazione Santa Lucia-IRCCS, Rome, Italy.

Abstract

Alzheimer's disease (AD) is a chronic neurodegenerative disorder characterized by specific patterns of gray and white matter damage and cognitive/behavioral manifestations. The cerebellum has also been implicated in the pathophysiology of AD. Because the cerebellum is known to have strong functional connectivity (FC) with associative cerebral cortex regions, it is possible to hypothesize that it is incorporated into intrinsic FC networks relevant to cognitive manifestation of AD. In the present study, the cerebellar dentate nucleus, the largest cerebellar nucleus and the major output channel to the cerebral cortex, was chosen as the region of interest to test potential cerebellocerebral FC alterations and correlations with patients' memory impairment in a group of patients with AD. Compared to controls, patients with AD showed an increase in FC between the dentate nucleus and regions of the lateral temporal lobe. This study demonstrates that lower memory performances in AD may be related to altered FC within specific cerebellocortical functional modules, thus suggesting the cerebellar contribution to AD pathophysiology and typical memory dysfunctions.

Keywords

Cerebellum

Alzheimer's disease

Functional connectivity

Dentate nucleus

Resting-state fMRI

Memory

1. Introduction

Alzheimer's disease (AD) is the most common form of cognitive decline in the elderly. In the typical form, it manifests with prominent deficits in episodic memory (Chan et al., 2009, Zhou et al., 2017), accompanied by progressive atrophy of the cerebral cortex with a distinct anatomical distribution (Braak and Braak, 1991). Consistently, pathological changes predominantly target the hippocampus, as well as medial temporal lobes, the bilateral posterior cingulate cortices, precuneus, and lateral temporoparietal lobes (Braak et al., 1993).

For a long time, the cerebellum has been thought to be spared by AD (Guo et al., 2016, Jacobs et al., 2018) and has received little attention in the context of AD's cognitive decline. More recently, clinical and neuroimaging evidence of the cerebellum's involvement in cognition, language, and emotion (Baumann and Mattingley, 2012, Clausi et al., 2017, Leggio and Olivito, 2018, Lupo et al., 2018, Schmahmann and Sherman, 1998), together with neuropathological and MRI studies that have shown cerebellar alterations in AD (Jacobs et al., 2018, Toniolo et al., 2018), has prompted increasing interest in this structure. The involvement of the vermis and posterior cerebellar lobe has been shown in the early stages, whereas extension to the anterior cerebellar lobe has been shown in more advanced stages of the disease (Jacobs et al., 2018). Consistently, Toniolo et al. (2018) also showed a progression of cerebellar gray matter (GM) volume changes throughout a continuous spectrum from early to late clinical stages of AD. Structurally, the cerebellum is connected to the cerebral cortex via topographically organized connections and, consequently, different parts of the cerebellum are connected with distinct cerebral regions. The largest structure linking the cerebellum to the rest of the brain is the dentate nucleus (DN) (Sultan et al., 2010), a cluster of excitatory neurons located within the deep white matter of each cerebellar hemisphere. The connections are known to be mainly contralateral and to be traditionally segregated in sensorimotor/cognitive functional modules (O'Reilly et al., 2010). This evidence has been widely documented, showing in particular a clear segregation between the “sensorimotor” and “cognitive” cerebellum. The former, located in the anterior lobe (lobules III-VI, and VIII), has connections with motor, somatosensory, visual, and auditory cortices (Kelly and Strick, 2003, Schmahmann, 1996, Schmahmann et al., 2004), whereas the latter, in the posterior lobe (lobules VIIa, Crus I, and II), has connections with prefrontal and posterior-parietal cortices related to cognition and emotion (Kelly and Strick, 2003, Ramnani, 2006). Accordingly, in addition to typical motor deficits (Takahashi et al., 2010), the presence of cognitive impairment has been shown in subjects with focal or degenerative cerebellar damage (Olivito et al., 2017a, Olivito et al., 2018, Schmahmann, 1998, Stoodley et al., 2016, Tedesco et al., 2011). Specifically, cerebellar cognitive impairment has been linked to a

functional alteration of cerebellocerebral interaction (Broich et al., 1987, Clausi et al., 2009, Komaba et al., 2000). Moreover, it has been recently shown that cerebellar dysfunctions may affect spatially separated regions of the brain and that cerebellar cognitive impairment could be related to abnormal functional connectivity (FC) patterns within specific cerebellocortical networks (Olivito et al., 2017b). FC is the mechanism underpinning the regional synchronous activation between spatially distributed brain areas, which is believed to mediate complex cognitive tasks (Damoiseaux et al., 2006) and can be easily measured by using resting-state functional MRI (RS-fMRI) (Biswal et al., 1997). Because connectivity-based approaches can map large-scale networks in health and detect the network-level alterations in disease, RS-fMRI has provided a great insight into understanding the neural substrate of cognitive dysfunctions in AD. Indeed, it has been suggested that neuronal dysfunctions in AD could be related not only to brain alterations at a regional level but also at the network level, causing a failure of functional coherence among specific brain regions (Greicius et al., 2004), especially when considering that a collective effort of different areas may be necessary to accomplish more complex functions. Thus, it is conceivable that FC alterations within specific cerebellocortical networks may also contribute to clinical symptoms observed in patients with AD. Recently, cerebellar GM loss has been related to cognitive dysfunctions in AD (Toniolo et al., 2018), whereas differences in FC between cerebellar and cerebral regions have not been specifically investigated.

From an anatomic point of view, the cortical cerebellar outputs converge onto DN, the largest cerebellar output channel, and, in turn, send neural fibers back to the cerebral cortex (Middleton and Strick, 1998). Thus, the hypothesis is that the cerebellar atrophy in AD may impact the functional activity of the DN and its excitatory modulation of target areas in the cerebral cortex. It is worth noting that, although FC is not identical to anatomical connectivity (Honey et al., 2009), the spatial pattern of resting-state FC is determined by the underlying anatomical connections (De Luca et al., 2006, Fox and Raichle, 2007, van den Heuvel et al., 2009, Wang et al., 2013). In light of this evidence, in the present study, we assessed for the first time potential alterations in FC between the DN and cerebral targets using RS-fMRI to test the pattern of cerebello-cerebral FC in AD and to assess whether a lack of FC within specific cerebellar-cerebral circuits could characterize AD pathophysiology.

2. Materials and methods

2.1. Participants

Seventy-eight patients with AD (mean age/SD: 73.54/6.4; M/F:33/45) were included in the study.

The diagnosis of probable AD was according to the clinical criteria of the National Institute of Neurological and Communicative Disorders and Stroke-Alzheimer's Disease and Related Disorders Association (McKhann et al., 1984, McKhann et al., 2011). All recruited participants with a Hachinski score (Hachinski et al., 1975) higher than 4 were excluded. Major systemic, psychiatric, and other neurological illnesses were also carefully investigated and excluded in all participants. Participants were all right-handed, as assessed by the Edinburgh Handedness Inventory (Büsch et al., 2010). In addition, 58 healthy subjects (HS) (mean

age/SD: 64.7/8.7); M/F: 26/32 with normal intellectual level and no history of neurological or psychiatric illness were recruited as the control group.

This research study was approved by the Ethics Committee of Santa Lucia Foundation, according to the principles expressed in the Declaration of Helsinki. Written informed consent was obtained from each subject.

2.2. MRI acquisition protocol

All patients with AD (=78) and HS (=58) underwent an MRI examination at 3T (Magnetom Allegra, Siemens, Erlangen, Germany) that included the following acquisitions: (1) dual-echo turbo spin echo [TSE] (TR = 6190 ms, TE = 12/109 ms); (2) fast-FLAIR (TR = 8170 ms, 204 TE = 96 ms, TI = 2100 ms); (3) T1-weighted 3D high-resolution scan 3D modified driven equilibrium Fourier transform [44] (TR = 1338 ms, TE = 2.4 ms, matrix = 256 × 224 × 176, in-plane FOV = 250 × 250 mm2, slice thickness = 1 mm); (4) T2*-weighted echo-planar imaging (EPI) sensitized to blood oxygenation level–dependent imaging contrast (TR, 2080 ms, TE 30 ms, 32 axial slices parallel to AC-PC line, matrix 64 × 64, pixel size 3 × 3 mm2, slice thickness 2.5 mm, flip angle 70°) for resting-state fMRI. Blood oxygenation level–dependent imaging echo planar images were collected during rest for a 7 minutes and 20 seconds period, resulting in a total of 220 volumes. During this acquisition, subjects were instructed to keep their eyes closed, not to think of anything in particular, and not to fall asleep. The TSE scans of patients, acquired as part of this research study, were reviewed by an expert neuroradiologist to characterize the brain anatomy and determine the presence of macroscopic structural abnormalities. Visual assessment of the medial temporal lobe atrophy (Scheltens et al., 1995) was performed on coronal 3D T1-weighted images to identify localized atrophy within the medial temporal region on each side. The score ranges from 0 (absence of atrophy) to 4 (marked atrophy) and is interpreted in relation to the age (<75 years: score 2 or more is abnormal; ≥75 years: score 3 or more is abnormal). For the HS group, conventional MRI was inspected to exclude any pathological conditions according to the inclusion criteria.

2.3. Resting-state fMRI data preprocessing

Data were preprocessed using Statistical Parametric Mapping version 8 [Wellcome Department of Imaging Neuroscience; SPM8 (http://www.fil.ion.ucl.ac.uk/spm/

)], and in-house software implemented in MATLAB (The Mathworks Inc, Natick, MA, USA). For each subject, the first 4 volumes of the fMRI series were discarded to allow for T1 equilibration effects. The preprocessing steps included correction for head motion, compensation for slice-dependent time shifts, normalization to the EPI template in MNI coordinates provided with SPM8, and smoothing with a 3D Gaussian Kernel with 8 mm3 full width at half maximum. For each data set, motion correction was checked by computing the average mean displacement as the root mean square of the 6 realignment parameters. Participants with a mean displacement larger than 1.3 mm were excluded. In addition, to minimize the risk that our results were affected by differing degrees of motion for the 2 participants' groups, we computed the average framewise displacement (FD, Power et al., 2012) and compared them between AD and HS using independent sample T-tests.

The global temporal drift was removed using a third-order polynomial fit, the signal was regressed against the realignment parameters, and then averaged over whole-brain voxels, to remove other potential sources of bias. Subsequently, all images were filtered by a phase-insensitive band-pass filter (pass band 0.01–0.08 Hz) to reduce the effect of low-frequency drift and high-frequency physiological noise. Considering that GM atrophy may affect FC (De Vico Fallani et al., 2014), every participant's modified driven equilibrium Fourier transform was segmented in SPM to estimate the total GM volume (absolute value) to be set as nuisance variable.

2.4. Neuropsychological assessment of memory functions

Owing to the retrospective nature of the study, neuropsychological (NPS) assessment exploring episodic memory functions was only available for 36 of patients with AD (mean age/SD: 73.7/3.6; M/F:11/25) and 32 of HS (mean age/SD: 69.3/7.1; M/F:15/17) (referred to as NPS group). The memory battery included the following tests: (1) verbal long-term memory: 15-Word List (immediate and 15-min delayed recall) (Carlesimo et al., 1996); Short Story Test (immediate and 20-min delayed recall) (Carlesimo et al., 2002); (2) visuospatial long-term memory: Complex Rey's Figure (immediate and 20-min delayed recall) (Carlesimo et al., 2002); (3) short-term verbal (digit span) and visuospatial memory (Corsi block-tapping task) (Monaco et al., 2013). The general cognitive efficiency was assessed by using Mini–Mental State Examination (MMSE) (Folstein et al., 1975). According to inclusion criteria, Raven's Colored Progressive Matrices (Raven, 1947) were used to ensure that HS had a normal intellectual level.

3. Statistical analysis

3.1. Definition of regions of interest and seed-based analyses

The left and right DN masks were separately extracted according to the spatially unbiased atlas template of the cerebellum and brainstem (Diedrichsen et al., 2009) (Fig. 1) and resliced into EPI standard space.

To estimate the correlation between each voxel in the brain and the seed regions, we used a first-level SPM model. The mean time course within each seed region of interest was extracted for every participant and used as a regressor in a first-level SPM analysis. The resulting beta images are thus equivalent to the Fisher z-transformed maps of the correlation coefficient. These images were taken to the second level, for a group analysis. At second level, the group-level main effect of seed-to-voxel connectivity was tested by means of the F-test of significance for both the left and right DN. Then, a two-sample t-test model was used to explore differences in connectivity between patients and controls in each region of interest. Age and the total GM volume were set as covariate of no interest. To control for the effect of gender distribution across group, sex was also set nuisance variable. Between-group statistical significance was set at $p < 0.05$ family-wise error (FWE)-corrected at cluster level (clusters formed with uncorrected voxels $p < 0.005$ at voxel level).

Results were masked by the group-level main effect ($p < 0.05$ uncorrected).

3.2. Neuropsychological assessment of memory functions

For each tests, individual raw scores were converted to obtain a mean z-score to evaluate patients' memory performances. Individual z-scores were calculated with reference to the control group using the following formula: (subject raw score − population mean)/population standard deviation (SD).

3.3. Behavioral correlations with functional connectivity

Based on RS-fMRI results, the mean dentate-cerebral FC values from clusters that were significantly altered in patients were extracted. The distribution of variables was tested by the Shapiro-Wilk test (Oztuna et al., 2006). Because scores at each test did not present a normal distribution ($p < 0.05$), non-normal distribution correlations between memory scores and FC value in patients with AD were performed by Spearman's test by means of SPSS statistics package. For the purpose of these correlations, individual NPS raw scores of each memory test (N = 10) were used. To avoid 1 type error, Bonferroni correction for multiple comparisons was fixed at $p = 0.005$ (= 0.05/10).

4. Results

4.1. Demographic and clinical characteristics

The visual MRI inspection of TSE scans and the age-dependent cutoff medial temporal lobe atrophy score showed the presence of atrophy within the medial temporal region of patients with AD (<75: 2.92). None of the HS had macroscopic brain alterations.

Thirteen participants with AD had to be removed because of excessive motion (see Section 4.2). Thus, the final MRI analysis included 65 AD participants (mean age/SD: 73.6/6.21; M/F: 28/37) and 58 HS (mean age/SD: 64.7/8.76; M/F: 26/32), whereas the final NPS group included 26 patients with AD (mean age/SD: 73.4/3; M/F: 8/18) and 30 HS (mean age/SD: 69.1/6.75; M/F: 17/13). The mean age of the groups included in the MRI analysis was significantly different (independent sample t-test: $t = -6.36$, $p = 0.000$), whereas no difference was found in terms of gender distribution ($X2 = 0.03$, $p = <0.05$). By contrast, the AD (N = 26) and HS groups (N = 30) of the NPS subsample did not differ in terms of age (independent sample t-test: $t = 0.41$, $p = <0.05$), education (independent sample t-test: $t = -1.67$, $p = <0.05$), and sex ($X2 = 3.78$, $p = <0.05$). As expected, MMSE scores showed that patients with AD (MMSE: <24) had lower general cognitive efficiency than controls (MMSE: >24), as also assessed by the t-test ($t = -6.61$, $p < 0.05$) (see also Table 1). As showed by the Raven's Colored Progressive Matrices score, HS had a normal intellectual level (mean age/SD: 31.7/3.2). Demographic data and MMSE scores of NPS group are summarized in Table 1.

4.2. Seed-based analysis

After computing the average mean displacement as the root mean square of the 6 realignment parameters, 13 of 78 AD participants with a mean displacement larger than 1.3 mm were removed. After removing 13 patients with AD, the average mean displacement was

0.63 (SD = 0.32) for the whole control group and 0.74 (SD = 0.34) for the whole AD group. The p-value estimated by a 2-sample t-test was 0.07. The average FD was 0.57 (SD = 0.31) for the controls and 0.63 for the AD (SD = 0.36), p = 0.32. When looking at the NPS subsamples, the average mean displacement was 0.64 (SD = 0.34) for controls and 0.62 (SD = 0.32) for AD, p = 0.85; the mean FD was 0.61 (SD = 0.34) for controls and 0.56 for AD (SD = 0.35), p-value = 0.6.

The main effect of left and right DN connectivity at rest is shown in Fig. 2A. Left and right DN showed a pattern of FC involving both ipsilateral and contralateral regions in the cerebral cortex (FWE 0.05 corrected at cluster level). Specifically, in the contralateral cerebral hemisphere, the left DN showed significant FC with the precuneus, the hippocampus, the inferior temporal gyrus, the temporal fusiform cortex, and the thalamus.

Regions in the ipsilateral cerebral hemisphere included the hippocampus and the parahippocampal gyrus, the superior frontal gyrus and frontal pole, the cingulate gyrus, the temporal fusiform cortex, and the lingual gyrus. In the contralateral cerebral hemisphere, the right DN showed significant FC with the temporal fusiform cortex, the precuneus, and the lingual gyrus. Regions in the ipsilateral cerebral hemisphere include the middle frontal gyrus and frontal pole, the thalamus, the caudate, the parahippocampal gyrus, and temporal fusiform cortex. Detailed statistics with peak voxels showing statistical significance in a cluster are reported in Table 2A and B. When comparing to HS, a selective pattern of FC differences was found between the left DN and contralateral regions of the right temporal and occipital lobe in patients with AD. Specifically, the main finding was a significant pattern of FC increase between the left DN and a set of regions including the inferior temporal pole, temporal planus/superior temporal gyrus, the temporo-occipital fusiform cortex, and lateral occipital cortex (FWE 0.05). In addition, a smaller cluster of increased FC was found between the right DN and left temporal fusiform cortex and left lateral occipital regions.

No regions of significantly decreased FC with left and right DN were found.

Regions of significantly increased FC with left and right DN are shown in Fig. 2B. Detailed statistics are reported in Table 3.

4.3. Neuropsychological assessment of memory functions

Performance raw data of AD and HS groups are reported in Table 4 expressed in mean and SD. The evaluation of memory profiles revealed that patients with AD had negative z-scores in all memory domains explored. In particular, (forward and backward) verbal short-term memory, (backward) visuospatial short-term memory, and (immediate) long-term visuospatial memory were −1, generally considered to indicate pathology. However, significantly worse performances were obtained in tests of (immediate and delayed) verbal long-term memory, (forward) visuospatial short-term memory, and (delayed) visuospatial long-term memory, as

indicated by scores approximating or lower than −3. A graphical representation of patients' performances is reported in Fig. 3 expressed in z-scores

4.4. Neuropsychological correlations with functional connectivity

Spearman's correlation coefficients revealed only one correlation between impaired memory performances in the (immediate) verbal long-term memory and FC right temporal fusiform cortex that did not survive after Bonferroni correction (15-word list; p = >0.005).

5. Discussion

The present RS-fMRI study provides the first evidence of altered FC between the DN and specific cerebral structures in patients with AD. In particular, a selective pattern of increased FC was found between the left DN and regions of the right temporal lobe, including inferior temporal pole, temporal planum and superior temporal gyrus, the temporo-occipital fusiform cortex, the right temporo-occipital pole, and the lateral occipital cortex. In addition, for the purpose of the present work, the relationship between dentato-cerebral FC and memory scores was investigated.

In line with the evidence that neuronal dysfunctions in AD could be related to a failure of functional coherence among specific brain regions (Greicius et al., 2004), it is possible to hypothesize that the disrupted functional interaction between the cerebellum and cerebral cortex could be also implicated in the pathophysiology of AD. Indeed, FC may provide further insight into understanding the neural substrate of AD.

At a regional level, medial and lateral temporal regions are the most affected cortical regions in AD (Frisoni et al., 2005; Hirata et al., 2005; Seeley et al., 2009), and episodic memory deficits are the most common cognitive symptoms associated with right temporal lobe atrophy (Chan et al., 2009).

More recently, neuroimaging evidence of cerebellar atrophy in AD has also emerged (Guo et al., 2016, Jacobs et al., 2018), involving in particular the posterior lobes (lobules VI and Crus I-II) (Toniolo et al., 2018), known to have strong FC with distinct associative cerebral regions (Habas et al., 2009, Olivito et al., 2017b). Specifically, the cortical cerebellar outputs converge onto the DN that, in turn, sends neural fibers back to the cerebral cortex (Middleton and Strick, 1998). Thus, cerebellocortical circuits could be selectively targeted by major degenerative disorders.

In the present study, we first assessed whole-brain cerebellar DN connectivity at rest and found a widespread pattern of connectivity involving bilateral cortical and subcortical brain regions (see Table 2 for details), including the hippocampus and parahippocampal formation. When compared with controls, patients with AD showed a specific pattern of hyperconnectivity between the DN and temporal (such as inferior temporal pole, superior temporal pole, and temporal planum) and occipital cerebral regions, indicating an increased neural synchronization between the cerebellum and these cerebral regions. The cerebellum is known to modulate the cortical activity (Di Lazzaro et al., 1994; Middleton and Strick, 1998). Indeed, the cerebellum is widely connected with cerebral regions at a functional level

(Buckner et al., 2011, Habas et al., 2009) and contributes to distinct functional networks related to higher-level functions also including the default mode network (DMN) (Habas et al., 2009). In particular, RS-fMRI studies in healthy adults have classified Crus I/II as the cerebellar counterparts of the DMN (Buckner et al., 2011, Habas et al., 2009, Krienen and Buckner, 2009). This intrinsic functional network, which can be derived from RS-fMRI (Buckner et al., 2005, Grecius et al., 2003), is known to be typically implicated in episodic memory (Buckner et al., 2005, Zysset et al., 2003) and has been shown to be functionally altered in AD brain (Seeley et al., 2009). It has been recently suggested that some regions in the temporal pole belong to a set of cerebral regions referred to as the "default mode regions" and described as the ventral subsystem of the DMN (Qi et al., 2018) comprising, among others, the hippocampal formation, and the parahippocampal cortex. This is in line with the pattern of DN FC found here.

Interestingly, the pattern of hyperconnectivity in AD mainly involved the cerebellar DN and regions in the lateral temporal cortex that are also affected in AD (Frisoni et al., 2005; Hirata et al., 2005).

According to the Cortical Reallocation Theory (Squire, 2004), although structures of the medial temporal lobe (the hippocampus and parahippocampal cortex) are known to be involved in memory retrieval after memories are stored (Alvarez and Squire, 1994), neural activity in the lateral temporal cortex plays a crucial role during encoding and differentiates information that is likely to be remembered or forgotten (Ezzyat et al., 2018). In particular, it has been shown that encoding activity within the lateral temporal cortex (including the middle portions of the inferior, middle, and superior temporal gyri) measured with fMRI (Kim, 2011) and intracranial electroencephalography (Burke et al., 2014) predicts memory performance.

As expected, patients with AD had impaired memory performances as showed by the negative z-scores.

Thus, it is conceivable that, as result of neurodegenerative process, the functional interaction between the cerebellar DN and some memory-related cortical regions could be affected (see also Olivito et al., 2017b), thus contributing to memory dysfunctions. Interestingly, differences in FC seem to resemble the spatial atrophy patterns seen in AD (Buckner et al., 2005, Grecius et al., 2003). Previous fMRI studies have mapped the pattern of atrophy in neurodegenerative dementias onto previously described intrinsic connectivity networks and found that in AD, atrophy in the cerebral cortex and the cerebellum occurs in the DMN (Guo et al., 2016). However, the pattern of hyperconnectivity we found here mainly involved cerebral regions of the inferior and lateral temporal pole consistent with the evidence that AD neurodegeneration has prominent effects also on these regions (Bakkour et al., 2013).

Together with previous findings of cerebellar atrophy in AD in concert with the pattern of cerebral GM abnormalities, the increased FC evidenced in the present study suggests a release of the inhibitory control, which is normally exerted by the cerebellar cortex on the DN, where the connections to the cerebral cortex originate from, which impairs optimization of functions in specific cerebellocerebral modules. Thus, the resulting increase of the DN excitatory output, via cerebello-thalamo-cortical pathways, might contribute to the cerebral

cortical dysfunction in areas critically implicated in determining AD cognitive symptoms, and specifically those related to memory.

The fact that we found a multifarious set of regions to be affected (including also regions that are not strictly related to memory, such as occipital regions) is probably due to the diffuse atrophy pattern that characterizes the AD-related neurodegeneration, in line with the evidence that the pattern of cerebello-cerebral functional alterations strongly resemble the spatial atrophy pattern observed in AD (Guo et al., 2016) and that, to support a single function, the functional integration of many specialized areas may be necessary (Friston, 2011). Furthermore, it has to be considered that the DN FC results may be also influenced by the presence of indirect connections that remain undetected by the FC analysis (Friston, 2011).

The participation of the cerebellum in several cognitive functions, also including verbal memory (Andreasen et al., 1995; Grasby et al., 1993), and visuospatial abilities (Parsons and Fox, 1997) is now widely accepted. Association between specific cerebellar regions and cognitive functions was first derived from functional MRI studies in HS (Stoodley and Schmahmann, 2009), and further supported by behavioral (Schmahmann, 1998, Tedesco et al., 2011) and neuroimaging studies (Clausi et al., 2009, Olivito et al., 2018, Stoodley et al., 2016) in cerebellar-damaged patients that showed a relation between cerebellar structural alterations and cognitive deficits. The hypothesis is that, as a consequence of the isolated cerebellar damage, the neurons of the connected cerebral regions undergo an alteration of the synaptic inputs that they normally receive from the cerebellum and this may induce a structural reorganization of these cortical neurons that also results in functional impairment (Clausi et al., 2009).

Only recently, cognitive dysfunctions in patients with AD have been associated to GM loss in posterior hemispheric cerebellar regions (lobule VIIa, crus I-crus II), thus providing clear evidence of the cerebellar contribution to AD clinical symptoms (Toniolo et al., 2018). Of course, it has to be taken into account that in major neurodegenerative diseases, such as AD, the cerebral GM is diffusively affected. Thus, the cerebellar alterations per se can be only partially responsible for the GM volume reductions, and cerebellar and cortical changes are more likely to occur concomitantly and influence each other. Consistently, Guo et al. (2016) showed that the cerebellum and interconnected cerebral nodes undergo concomitant degenerative atrophy within the same functional module. Based on their results, authors suggested that the network-selective vulnerability could underlie the pathogenesis of neurodegeneration in both the cerebral and cerebellar cortices. This view supports the idea that the integrity of the entire circuit, including both cortical and subcortical structures, is the key to support healthy mental states (Schmahmann, 2016).

FC alterations in dentate-cerebral networks had never been related to cognitive deficits in AD, and this study represents the first step in the effort to dissect the complex functional interaction between the cerebellum and cerebral cortex in contributing to AD cognitive symptoms, and specifically memory. It has to be underlined that we did not find significant correlations between DN FC patterns and patients' memory scores. In spite of this, the consistency between the present findings and the existing research supports the significance of the conclusions. Specifically, our hypothesis is that, in our AD sample, functional

hyperconnectivity is the pathological manifestation of altered functional interaction between the DN and temporal cerebral regions. In line with our results, we conclude that hyperconnectivity between the DN and cerebral cortex may be a specific marker of reduced memory performances in patients with AD.

To conclude, there are some concerns that merit being discussed. Although the present results may represent a preliminary evidence of the cerebellar contribution to memory deficits in AD, it remains to be clarified how the cerebellum specifically intervenes in this memory processing. The striking microanatomical homogeneity of the cerebellum suggests a corresponding unity of function across motor and nonmotor domains (Ramnani, 2006) and has inspired the idea that the theories developed for motor control should also be informative for understanding cerebellar contributions to cognition. In line with the cerebellar sequencing hypothesis (Leggio and Molinari, 2015), the cerebellum may contribute to memory functions by comparing activity patterns to compute discrepancies, in the same way as motor and other cognitive domains (Brunamonti et al., 2014, Clausi et al., 2019, Leggio et al., 2011, Molinari et al., 2009).

In the context of motor control, it has been widely accepted that the cerebellum contributes during sequence acquisition rather than execution (Manto et al., 2012. Thus, in line with the evidence that DN functional alteration mainly affects lateral temporal regions involved in encoding stimuli that have to be remembered, the cerebellum may contribute by comparing, via distinct cerebellar subregions, the output of subvocal articulation with acoustically based phonological representations in a short-term store (Desmond et al., 1997).

However, testing this hypothesis goes beyond the scope of the present work and has not been specifically investigated.

Another limitation is that we did not specifically look at cerebellar and cerebral atrophy patterns in our cohort. However, the consistency between existing research and the present cognitive and functional results strongly support the general conclusions. Future investigations aiming to specifically assess these issues may shed further light and overcome these limitations.

Disclosure statement

The authors declare that the research was conducted in the absence of any commercial or financial relationships that could be construed as a potential conflict of interest.

Acknowledgements

This research was in part financially supported by Italian Ministry of Health, Italy (Linea di Ricerca Corrente: Neuroriabilitazione Cognitiva, Motoria e Neuroimmagini). Project Title: Ruolo del cervelletto nella patologia di Alzheimer a diverso stadio evolutivo.

References

Alvarez, P., Squire, L.R., 1994. Memory consolidation and the medial temporal lobe: a simple network model. Proc. Natl. Acad. Sci. U. S. A. 91, 7041e7045.

Andreasen, N.C., O'Leary, D.S., Arndt, S., Cizadlo, T., Hurtig, R., Rezai, K., Watkins, G.L., Ponto, L.L., Hichwa, R.D., 1995. Short-term and long-term verbal memory: a positron emission tomography study. Proc. Natl. Acad. Sci. U S A 92, 5111e5115.

Bakkour, A., Morris, J.C., Wolk, D.A., Dickersona, B.C., 2013. The effects of aging and Alzheimer's disease on cerebral cortical anatomy: specificity and differential relationships with cognition. Neuroimage 76, 332e344.

Baumann, O., Mattingley, J.B., 2012. Functional topography of primary emotion processing in the human cerebellum. Neuroimage 61, 805e811.

Biswal, B.B., Van Kylen, J., Hyde, J.S., 1997. Simultaneous assessment of flow and BOLD signals in resting-state functional connectivity maps. NMR Biomed. 10, 165e170.

Braak, H., Braak, E., Bohl, J., 1993. Staging of Alzheimer-related cortical destruction. Eur. Neurol. 33, 403e408.

Braak, H., Braak, E., 1991. Neuropathological staging of Alzheimer-related changes. Acta Neuropathol. 82, 239e259.

Broich, K., Hartmann, A., Biersack, H.J., Horn, R., 1987. Crossed cerebello-cerebral diaschisis in a patient with cerebellar infarction. Neurosci. Lett. 83, 7e12.

Brunamonti, E., Chiricozzi, F.R., Clausi, S., Olivito, G., Giusti, M.A., Molinari, M., Ferraina, S., Leggio, M., 2014. Cerebellar damage impairs executive control and monitoring of movement generation. PLoS One 9, e85997.

Buckner, R.L., Krienen, F.M., Castellanos, A., Diaz, J.C., Yeo, B.T., 2011. The organization of the human cerebellum estimated by intrinsic functional connectivity. J. Neurophysiol. 106, 2322e2345.

Buckner, R.L., Snyder, A.Z., Shannon, B.J., LaRossa, G., Sachs, R., Fotenos, A.F., Sheline, Y.I., Klunk, W.E., Mathis, C.A., Morris, J.C., Mintun, M.A., 2005. Molecular, structural, and functional characterization of Alzheimer's disease: evidence for a relationship between default activity, amyloid, and memory. J. Neurosci.

25, 7709e7717.
Burke, J.F., Long, N.M., Zaghloul, K.A., Sharan, A.D., Sperling, M.R., Kahana, M.J., 2014. Human intracranial high-frequency activity maps episodic memory formation in space and time. Neuroimage 85, 834e843.
Büsch, D., Hagemann, N., Bender, N., 2010. The dimensionality of the Edinburgh Handedness Inventory: an analysis with models of the item response theory. Laterality 15, 610e628.
Carlesimo, G.A., Buccione, I., Fadda, L., Graceffa, A., Mauri, M., Lorusso, S., Bevilacqua, G., Caltagirone, C., 2002. Standardizzazione di due test di memoria per uso clinico: Breve Racconto e Figura di Rey. Nuova Rivista di Neurologia 12, 1e13.
Carlesimo, G.A., Caltagirone, C., Gainotti, G., Fadda, L., Gallassi, R., Lorusso, S., Marfia, G., Marra, C., Nocentini, U., Parnetti, L., 1996. The mental deterioration battery: normative data, diagnostic reliability and qualitative analyses of cognitive impairment. Eur. Neurol. 36, 378e384.
Chan, D., Anderson, V., Pijnenburg, Y., Whitwell, J., Barnes, J., Scahill, R., Stevens, J.M., Barkhof, F., Scheltens, P., Rossor, M.N., Fox, N.C., 2009. The clinical profile of right temporal lobe atrophy. Brain 132 (Pt 5), 1287e1298.
Clausi, S., Iacobacci, C., Lupo, M., Olivito, G., Molinari, M., Leggio, M., 2017. The role of the cerebellum in unconscious and conscious processing of emotions: a review. Appl. Sci. 7, 521.
Clausi, S., Bozzali, M., Leggio, M.G., Di Paola, M., Hagberg, G.E., Caltagirone, C., Molinari, M., 2009. Quantification of gray matter changes in the cerebral cortex after isolated cerebellar damage: a voxel-based morphometry study. Neuro-science 162, 827e835.
Clausi, S., Olivito, G., Lupo, M., Siciliano, L., Bozzali, M., Leggio, M., 2019. The cere-bellar predictions for social interactions: theory of mind abilities in patients with degenerative cerebellar atrophy. Front Cell Neurosci 8, 510.
Damoiseaux, J.S., Rombouts, S.A., Barkhof, F., Scheltens, P., Stam, C.J., Smith, S.M., Beckmann, C.F., 2006. Consistent resting-state networks across healthy subjects.

Proc. Natl. Acad. Sci. U. S. A. 103, 13848e13853.
De Luca, M., Beckmann, C.F., De Stefano, N., Matthews, P.M., Smith, S.M., 2006. fMRI resting state networks define distinct modes of long-distance interactions in the human brain. Neuroimage 29, 1359e1367.
G. Olivito et al. / Neurobiology of Aging 89 (2020) 32e40 39
De Vico Fallani, F., Richiardi, J., Chavez, M., Achard, S., 2014. Graph analysis of functional brain networks: practical issues in translational neuroscience. Philos. Trans. R. Soc. Lond. B Biol. Sci. 369, 1653.
Desmond, J.E., Gabrieli, J.D., Wagner, A.D., Ginier, B.L., Glover, G.H., 1997. Lobular patterns of cerebellar activation in verbal working memory and finger tapping tasks as revealed by functional MRI. J. Neurosci 17, 9675e9685.
Di Lazzaro, V., Restuccia, D., Molinari, M., Leggio, M., Nardone, R., Fogli, D., Tonali, P., 1994. Excitability of the motor cortex to magnetic stimulation in patients with cerebellar lesions. J. Neurol. Neurosurg. Psychiatry 57, 108e110.
Diedrichsen, J., Balsters, J.H., Flavell, J., Cussans, E., Ramnani, N., 2009. A probabilistic atlas of the human cerebellum. Neuroimage 46, 39e46.
Ezzyat, Y., Wanda, P.A., Levy, D.F., Kadel, A., Aka, A., Pedisich, I., Sperling, M.R., Sharan, A.D., Lega, B.C., Burks, A., Gross, R.E., Inman, C.S., Jobst, B.C., Gorenstein, M.A., Davis, K.A., Worrell, G.A., Kucewicz, M.T., Stein, J.M., Gorniak, R., Das, S.R., Rizzuto, D.S., Kahana, M.J., 2018. Closed-loop stimulation of temporal cortex rescues functional networks and improves memory. Nat. Commun. 9, 365.
Folstein, M.F., Folstein, S.E., McHugh, P.R., 1975. “Mini-mental state”. A practical method for grading the cognitive state of patients for the clinician. J. Psychiatr. Res. 12, 189e198.
Fox, M.D., Raichle, M.E., 2007. Spontaneous fluctuations in brain activity observed with functional magnetic resonance imaging. Nat. Rev. Neurosci. 8, 700e711.
Frisoni, G.B., Testa, C., Sabattoli, F., Beltramello, A., Soininen, H., Laakso, M.P., 2005. Structural correlates of early and late onset Alzheimer's disease: voxel based morphometric study. J. Neurol. Neurosurg. Psychiatry 76, 112e114.

Friston, K.J., 2011. Functional and effective connectivity: a review. Brain Connect. 1, 13e36.

Grasby, P.M., Frith, C.D., Friston, K.J., Bench, C., Frackowiak, R.S., Dolan, R.J., 1993. Functional mapping of brain areas implicated in auditoryeverbal memory function. Brain 116, 1e20.

Grecius, M.D., Krasnow, B., Reiss, A.L., Menon, V., 2003. Functional connectivity in the resting brain: a network analysis of the default mode hypothesis. Proc. Natl. Acad. Sci. U. S. A. 100, 253e258.

Greicius, M.D., Srivastava, G., Reiss, A.L., Menon, V., 2004. Default mode network activity distinguishes Alzheimer's disease from healthy aging: evidence from functional MRI. Proc. Natl. Acad. Sci. U. S. A. 101, 4637e4642.

Guo, C.C., Tan, R., Hodges, J.R., Hu, X., Saber, S., Hornberger, M., 2016. Network-selective vulnerability of the human cerebellum to Alzheimer's disease and frontotemporal dementia. Brain 139, 1532e1543.

Habas, C., Kamdar, N., Nguyen, D., Prater, K., Beckmann, C.F., Menon, V., Greicius, M.D., 2009. Distinct cerebellar contributions to intrinsic connectivity networks. J. Neurosci. 29, 8586e8594.

Hachinski, V.C., Iliff, L.D., Zilhka, E., Du Boulay, G.H., McAllister, V.L., Marshall, J., Russell, R.W., Symon, L., 1975. Cerebral blood flow in dementia. Arch. Neurol. 32, 632e637.

Hirata, Y., Matsuda, H., Nemoto, K., Ohnishi, T., Hirao, K., Yamashita, F., Asada, T., Iwabuchi, S., Samejima, H., 2005. Voxel-based morphometry to discriminate early Alzheimer's disease from controls. Neurosci. Lett. 382, 269e274.

Honey, C.J., Sporns, O., Cammoun, L., Gigandet, X., Thiran, J.P., Meuli, R., Hagmann, P., 2009. Predicting human resting-state functional connectivity from structural connectivity. Proc. Natl. Acad. Sci. U. S. A. 106, 2035e2040.

Jacobs, H.I.L., Hopkins, D.A., Mayrhofer, H.C., Bruner, E., van Leeuwen, F.W., Raaijmakers, W., Schmahmann, J.D., 2018. The cerebellum in Alzheimer's disease: evaluating its role in cognitive decline. Brain 141, 37e47.

Kelly, R.M., Strick, P.L., 2003. Cerebellar loops with motor cortex and prefrontal

cortex of a nonhuman primate. J. Neurosci. 23, 8432e8444.
Kim, H., 2011. Neural activity that predicts subsequent memory and forgetting: a meta-analysis of 74 fMRI studies. Neuroimage 54, 2446e2461.
Komaba, Y., Osono, E., Kitamura, S., Katayama, Y., 2000. Crossed cerebellocerebral diaschisis in patients with cerebellar stroke. Acta Neurol. Scand. 101, 8e12.
Krienen, F.M., Buckner, R.L., 2009. Segregated fronto-cerebellar circuits revealed by intrinsic functional connectivity. Cereb. Cortex 19, 2485e2497.
Leggio, M., Molinari, M., 2015. Cerebellar sequencing: a trick for predicting the future. Cerebellum 14, 35e38.
Leggio, M.G., Chiricozzi, F.R., Clausi, S., Tedesco, A.M., Molinari, M., 2011. The neuropsychological profile of cerebellar damage: the sequencing hypothesis. Cortex 47, 137e144.
Leggio, M., Olivito, G., 2018. Topography of the cerebellum in relation to social brain regions and emotions. Handbook of Clinical Neurology, 154. Elsevier B.V., pp. 71e84
Lupo, M., Olivito, G., Siciliano, L., Masciullo, M., Bozzali, M., Molinari, M., Leggio, M., 2018. Development of a psychiatric disorder linked to cerebellar lesions. Cerebellum 17, 438e446.
Manto, M., Bower, J.M., Conforto, A.B., Delgado-García, J.M., da Guarda, S.N., Gerwig, M., Habas, C., Hagura, N., Ivry, R.B., Mariën, P., Molinari, M., Naito, E., Nowak, D.A., Oulad Ben Taib, N., Pelisson, D., Tesche, C.D., Tilikete, C., Timmann, D., 2012. Consensus paper: roles of the cerebellum in motor control–the diversity of ideas on cerebellar involvement in movement. Cerebellum 11, 457e487.
McKhann, G., Drachman, D., Folstein, M., Katzman, R., Price, D., Stadlan, E.M., 1984. Clinical diagnosis of Alzheimer's disease: report of the NINCDS-ADRDA Work Group under the auspices of Department of Health and Human Services Task Force on Alzheimer's Disease. Neurology 34, 939e944.
McKhann, G., Knopman, D., Chertkow, H., Hymann, B., Jack, C.R., Kawas, C., Klunk, W.E., Koroshetz, W.J., Manly, J.J., Mayeux, R., Mohs, R.C., Morris, J.C.,

Rossor, M.N., Scheltens, P., Carrillo, M.C., Thies, B., Weintraub, S., Phelps, C.H., 2011. The diagnosis of dementia due to Alzheimer's disease: recommendations from the National Institute on aging- Alzheimer's association workgroups on diagnostic guidelines for Alzheimer's disease. Alzheimers Dement. 7, 263e269.
Middleton, F.A., Strick, P.L., 1998. Cerebellar output: motor and cognitive channels. Trends Cogn. Sci. 2, 348e354.
Molinari, M., Restuccia, D., Leggio, M.G., 2009. State estimation, response prediction, and cerebellar sensory processing for behavioral control. Cerebellum 8, 399e402.
Monaco, M., Costa, A., Caltagirone, C., Carlesimo, G.A., 2013. Forward and backward span for verbal and visuo-spatial data: standardization and normative data from an Italian adult population. Neurol. Sci. 34, 749e754.
O'Reilly, J.X., Beckmann, C.F., Tomassini, V., Ramnani, N., Johansen-Berg, H., 2010. Distinct and overlapping functional zones in the cerebellum defined by resting state functional connectivity. Cereb. Cortex 20, 953e965.
Olivito, G., Cercignani, M., Lupo, M., Iacobacci, C., Clausi, S., Romano, S., Masciullo, M., Molinari, M., Bozzali, M., Leggio, M., 2017b. Neural substrates of motor and cognitive dysfunctions in SCA2 patients: a network based statistics analysis. Neuroimage Clin. 14, 719e725.
Olivito, G., Lupo, M., Iacobacci, C., Clausi, S., Romano, S., Masciullo, M., Molinari, M., Cercignani, M., Bozzali, M., Leggio, M., 2017a. Microstructural MRI basis of the cognitive functions in patients with Spinocerebellar ataxia type 2. Neuroscience 366, 44e53.
Olivito, G., Lupo, M., Iacobacci, C., Clausi, S., Romano, S., Masciullo, M., Molinari, M., Cercignani, M., Bozzali, M., Leggio, M., 2018. Structural cerebellar correlates of cognitive functions in spinocerebellar ataxia type 2. J. Neurol. 265, 597e606.
Oztuna, D., Elhan, A.H., Tuccar, E., 2006. Investigation of pour different normality tests in terms of type I error rate and power under different distributions. Turkish J. Med. Sci. 36, 171e176.
Parsons, L.M., Fox, P.T., 1997. Sensory and cognitive functions. In: Schmahmann, J.D. (Ed.), The Cerebellum and Cognition. International Review of Neurobiology, Vol.

41. Academic Press, San Diego, pp. 255e271.
Power, J.D., Barnes, K.A., Snyder, A.Z., Schlaggar, B.L., Petersen, S.E., 2012. Spurious but systematic correlations in functional connectivity MRI networks arise from subject motion. Neuroimage 59, 2142e2154.
Qi, H., Liu, H., Hu, H., He, H., Zhao, X., 2018. Primary disruption of the memory-related subsystems of the default mode network in Alzheimer's disease: resting-state functional connectivity MRI study. Front Aging Neurosci. 10, 344.
Ramnani, N., 2006. The primate cortico-cerebellar system: anatomy and function. Nat. Rev. Neurosci. 7, 511e522.
Raven, J.C., 1947. Progressive Matrices, Sets A, Ab, B: Board and Book Forms. Lewis, London.
Scheltens, P., Launer, L.J., Barkhof, F., Weinstein, H.C., van Gool, W.A., 1995. Visual assessment of medial temporal lobe atrophy on magnetic resonance imaging: interobserver reliability. J. Neurol. 242, 557e560.
Schmahmann, J.D., 1998. Dysmetria of thought: clinical consequences of cerebellar dysfunction on cognition and affect. Trends Cogn. Sci. 2, 362e371.
Schmahmann, J.D., Ko, R., MacMore, J., 2004. The human basis pontis: motor syndromes and topographic organization. Brain 127 (Pt 6), 1269e1291.
Schmahmann, J.D., Sherman, J.C., 1998. The cerebellar cognitive affective syndrome. Brain 121, 561e579.
Schmahmann, J.D., 2016. Cerebellum in Alzheimer's disease and frontotemporal dementia: not a silent bystander. Brain 139 (Pt 5), 1314e1318.
Schmahmann, J.D., 1996. From movement to thought: anatomic substrates of the cerebellar contribution to cognitive processing. Hum. Brain Mapp. 4, 174e198.
Seeley, W.W., Crawford, R.K., Zhou, J., Miller, B.L., Greicius, M.D., 2009. Neurodegenerative diseases target large-scale human brain networks. Neuron 62, 42e52.
Squire, R.L., 2004. Memory systems of the brain: A brief history and current perspective. Neurobiol. Learn. Mem. 82, 171e177.
Stoodley, C.J., MacMore, J.P., Makris, N., Sherman, J.C., Schmahmann, J.D., 2016.

Location of lesion determines motor vs. cognitive consequences in patients with cerebellar stroke. Neuroimage Clin. 12, 765e775.
Stoodley, C.J., Schmahmann, J.D., 2009. Functional topography in the human cerebellum: a meta-analysis of neuroimaging studies. Neuroimage 44, 489e501.
Sultan, F., Hamodeh, S., Baizer, J.S., 2010. The human dentate nucleus: a complex shape untangled. Neuroscience 167, 965e968.
Takahashi, T., Katada, S., Onodera, O., 2010. Polyglutamine diseases: where does toxicity come from? What is toxicity? Where are we going? J. Mol. Cell Biol 2, 180e191.
Tedesco, A.M., Chiricozzi, F.R., Clausi, S., Lupo, M., Molinari, M., Leggio, M.G., 2011. The cerebellar cognitive profile. Brain 134, 3672e3686.
Toniolo, S., Serra, L., Olivito, G., Marra, C., Bozzali, M., Cercignani, M., 2018. Patterns of cerebellar gray matter atrophy across Alzheimer's disease progression. Front Cell Neurosci 12, 430.
van den Heuvel, M.P., Mandl, R.C., Kahn, R.S., Hulshoff Pol, H.E., 2009. Functionally linked resting-state networks reflect the underlying structural connectivity architecture of the human brain. Hum. Brain Mapp. 30, 3127e3141.
Wang, Z., Chen, L.M., Negyessy, L., Friedman, R.M., Mishra, A., Gore, J.C., Roe, A.W., 2013. The relationship of anatomical and functional connectivity to resting-state connectivity in primate somatosensory cortex. Neuron 78, 1116e1126.
Zhou, J., Liu, S., Ng, K.K., Wang, J., 2017. Applications of resting-state functional connectivity to neurodegenerative disease. Neuroimaging Clin. N. Am. 27, 663e683.
Zysset, S., Huber, O., Samson, A., Ferstl, E.C., von Cramon, D.Y., 2003. Functional specialization within the anterior medial prefrontal cortex: a functional magnetic resonance imaging study with human subjects. Neurosci. Lett. 335, 183e186

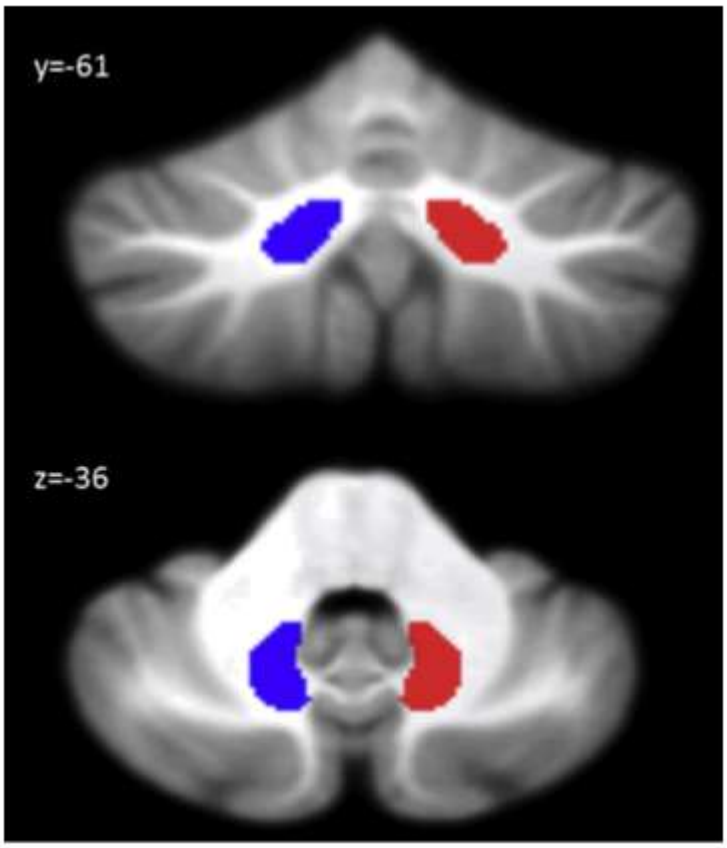

Figure 1. Seed region in the cerebellar dentate nucleus. Coronal (y) and axial (z) view of the generated left (blue) and right (red) dentate nucleus superimposed to the spatially unbiased atlas template of the cerebellum and brainstem (SUIT, Diedrichsen et al., 2009)

Demographic and clinical data	NPS group	
	AD (N = 26)	HS (N = 30)
	(Mean/SD)	
Age	74.5/2.2	69.3/7.1
Sex (M/F)	8/18	17/13
Education	10.8/3.4	12.4/3.5
MMSE[a]	18.9/3.1	28.9/1.4

Key: M, male; F, female; MMSE, Mini–Mental State Examination; AD, Alzheimer's disease; HS, healthy subject; NPS, neuropsychological.

[a] Scores corrected according to age and education presenting significant difference between groups.

Table 1Demographic data and MMSE scores of AD and HS group included for the neuropsychological analysis

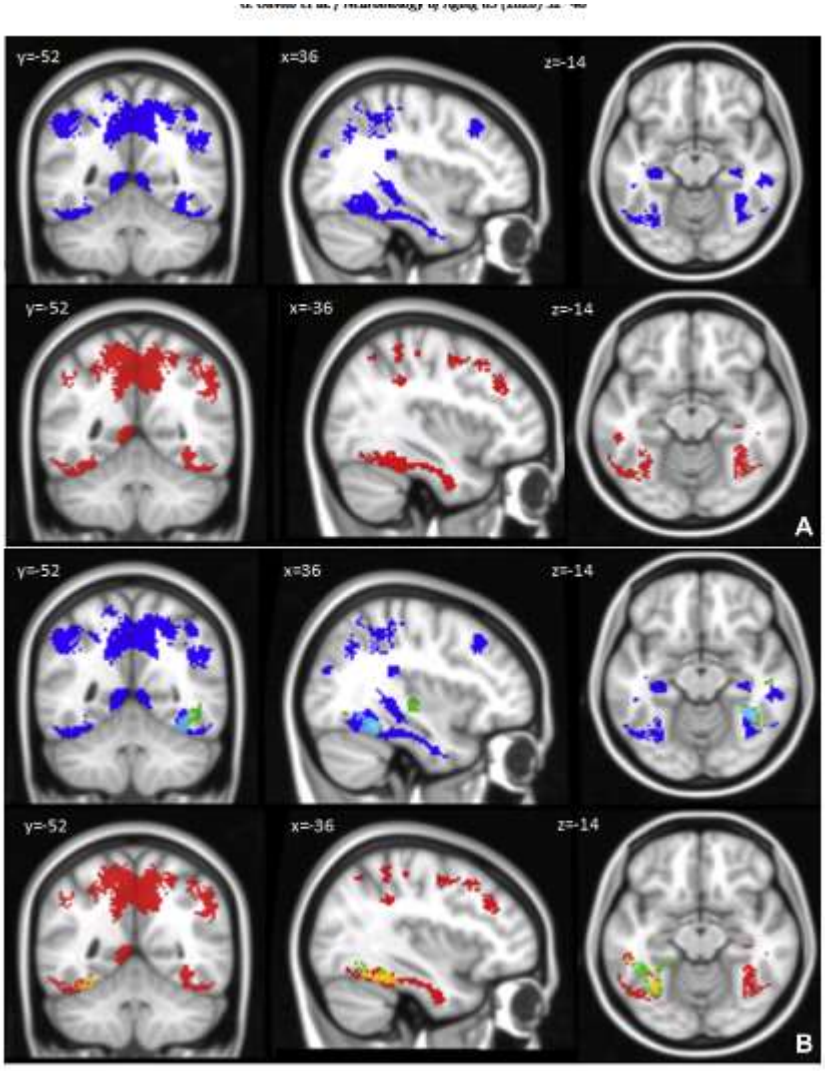

igure 2. (AeB) Patterns of dentate functional connectivity with the cerebral cortex. (A) Seed-to-voxel main effect is shown for left (in blue) and right (in red) DN functional

connectivity. Coronal (y), sagittal (x), and axial slices (z) in the Montreal Neurological Institute space. (B) Left (top panel) and right (bottom panel) increased dentate-cerebral

functional connectivity in AD compared with HS (in green) are shown in coronal (y), sagittal (x), and axial slices (z). X, Y, Z in the Montreal Neurological Institute space. Regions

overlapping with cerebral cluster of left and right DN main effect connectivity are shown in cyan and yellow, respectively. Clusters of increased FC in the cerebral cortex were

considered significant after correction for multiple comparisons (FWE-corrected $p < 0.05$). Images are shown in neurological convention. See Tables 2 and 3 for detailed statistics.

Abbreviations: DN, dentate nucleus; AD, Alzheimer's disease; HS, healthy subject; FC, functional connectivity

Seed	Cluster size (NoV)	Coordinates			Cluster peak Z-score	Brain region
		x	y	z		
(A) L-DN	9979	6	−52	50	6.78	R-Precuneus
		14	−52	52	6.62	R-Precuneus
		34	−34	−4	6.53	R-Hippocampus
	4231	16	50	34	6.71	R-Frontal pole
		−12	52	32	6.68	L-Frontal pole
		−6	48	38	6.00	L-Superior frontal gyrus
	1240	−34	−12	−30	>7	L-Parahippocampal gyrus
		−26	−14	−26	>7	L-Hippocampus
		−34	−12	−30	7.61	L-Parahippocampal gyrus
	1216	−30	−10	−30	>7	L-Parahippocampal gyrus
		34	−22	−26	>7	R-Temporal fusiform cortex
		52	−56	−20	7.08	R-Inferior temporal gyrus
	247	−8	−50	2	5.30	L- Cingulate gyrus, posterior division
		−14	−46	−6	4.01	L-Lingual gyrus
	208	−34	−30	−10	5.29	L-Hippocampus
		−22	−32	−8	3.78	L-Hippocampus
	122	8	−14	−4	5.89	R-Thalamus
(B) R-DN	6896	4	−46	54	7.81	R-Precuneus
		8	−76	42	6.71	R-Precuneus
		−8	−48	46	6.59	L-Precuneus
	4399	32	30	38	7.46	R-Middle frontal gyrus
		24	38	38	6.94	R-Frontal pole
		10	56	28	6.53	R-Frontal pole
	2346	18	−26	14	5.39	R-Thalamus
		12	18	8	5.37	R-Caudate
	1111	28	−10	−30	>7	R-Parahippocampal gyrus
		32	−20	−26	>7	R-Parahippocampal gyrus
		36	−6	−36	>7	R-Temporal fusiform cortex
	1085	−38	−12	−32	>7	L-Temporal fusiform cortex
		−34	−8	−38	7.21	L-Temporal fusiform cortex
		−36	−24	−24	7.08	L-Temporal fusiform cortex
	222	−8	−48	2	5.25	L-Lingual gyrus

MNI coordinates (x, y, and z) in the Montreal Neurological Institute space and peak Z-score of the peak voxels showing greatest statistical differences in a cluster are reported. Only regions that survived after correction for multiple comparisons (FWE-corrected $p < 0.05$) have been considered.
Key: NoV, number of voxels; L, left; R, right; MNI, Montreal Neurological Institute; DN, dentate nucleus.

Table 2

Statistics of seed-to-voxel main effect for left (L-) (A) and right (R-) (B) DN functional connectivity

Seed	Cluster size (NoV)	Coordinates			Cluster Peak Z-score	Brain region
		x	y	z		
L-DN	616	58	−18	2	3.64	R-Superior temporal gyrus
		38	−20	−6	3.61	R-Planum
		66	−30	6	3.50	R-Superior temporal gyrus
	500	40	−70	−2	4.07	R-Lateral occipital cortex
		42	−60	−6	4.06	R-Inferior temporal gyrus
		34	−46	−18	3.92	R-Temporo-occipital fusiform cortex
R-DN	442	−44	−44	−16	3.71	L-Temporal fusiform cortex
		−32	−54	−18	3.69	L-Temporo-occipital fusiform
		−42	−64	−8	3.34	L-Lateral occipital cortex

MNI coordinates (x, y, z) in the Montreal Neurological Institute space and peak Z-score of the peak voxels showing greatest statistical differences in a cluster are reported. Only regions that survived after correction for multiple comparisons (FWE-corrected $p < 0.05$) have been considered.
Key: AD, Alzheimer's disease; HS, healthy subject; NoV, number of voxels; L, left; R, right; DN, dentate nucleus.

Table 3

Statistics of left (L-) and right (R-) DN functional connectivity results (AD > HS)

Group	Cases	Rey_I	Rey_D	HRey_I	Frey_D	DS_For	DS_Back	Corsi_For	Corsi_Back	Sst_I	Sst_D
AD	26	17.5 (7.37)	1.23 (1.34)	2.4 (3.1)	2.1 (2.8)	4.8 (1.5)	2.8 (1.5)	2.9 (1.5)	2.3 (2)	2.1 (2.1)	1 (1.8)
HS	30	39.8 (9.4)	8.13 (2.21)	15 (6.3)	15.4 (5.6)	6.2 (1.2)	4.4 (0.7)	5 (0.9)	4.5 (0.9)	5.9 (1.3)	5.7 (1.2)

For each test, mean and standard deviation (SD) of raw scores are reported. Rey_I: 15-Word List (immediate recall); Rey_D: 15-Word List (delayed recall); DS_For: Digit Span forward; DS_Back: Digit Span Backward: Corsi_For: Corsi block-tapping test forward; Corsi_Back: Corsi block-tapping test backward; Frey_I: Complex Rey's Figure (immediate recall); Frey_D: Complex Rey's Figure (delayed recall); Sst_I: short story test (immediate recall); Sst_D: short story test (delayed recall).
Key: AD, Alzheimer's disease; HS, healthy subject; NPS, neuropsychological.

Table 4

Memory performance data of patients with AD and HS of the NPS group

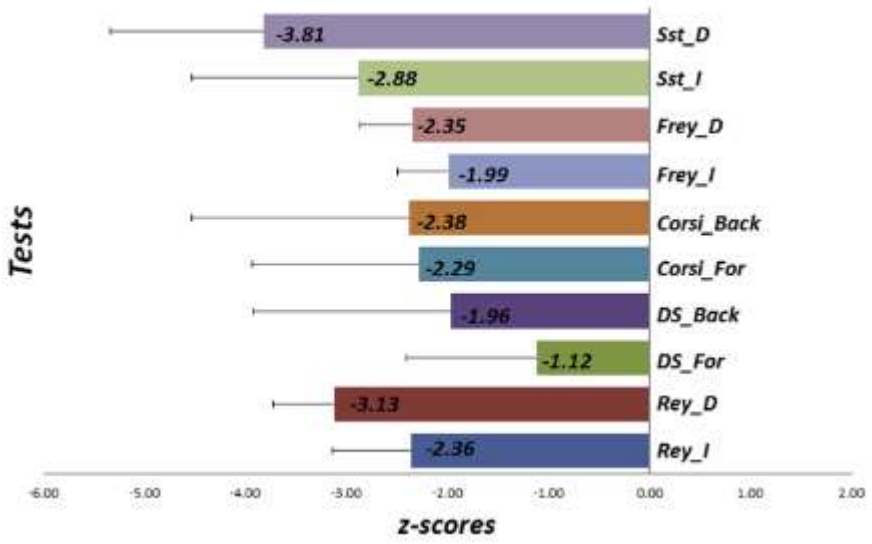

Fig. 3. Graphical representation of patients' performances expressed in z-scores. Patients had negative z-scores in all memory components explored. Rey_I: 15-Word List (im-

mediate recall); Rey_D: 15-Word List (delayed recall); DS_For: digit span forward; DS_Back: digit span backward: Corsi_For: Corsi block-tapping test forward; Corsi_Back: Corsi

block-tapping test backward; Frey_I: Complex Rey's Figure (immediate recall); Frey_D: Complex Rey's Figure (delayed recall); Sst_I: short story test (immediate recall); Sst_D: shortstory test (delayed recall).